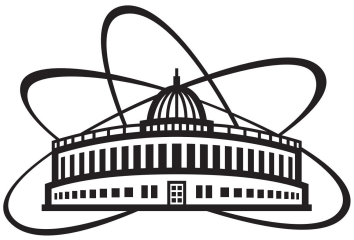

JOINT INSTITUTE FOR NUCLEAR RESEARCH
Veksler and Baldin laboratory of High Energy Physics

FINAL REPORT ON THE START PROGRAMME

Study of bulk properties of the medium produced in heavy ion collisions at MPD

Supervisor:
Dr Alexey Aparin
Student:
Anil Sharma
UGC-DAE CSR Kolkata Center
(University of Calcutta)
Participation Period:
October-November,
Summer Session, 2023

Dubna, Russia - 2023

DECLARATION

I, **Anil Sharma**, declare that the work presented in the project report titled "**Study of bulk properties of the medium produced in heavy ion collisions at MPD**" is my original work from **October to November 2023** and has not been submitted elsewhere for academic credit or publication. It has been carried out by me under the guidance of **Dr Alexey Aparin**, at Joint Institute for Nuclear Research, Veksler and Baldin laboratory of High Energy Physics.

I assert that all information and sources used in this project are accurately cited in the reference section, and I have given credit to all authors and contributors as appropriate.

I declare that I have adhered to ethical guidelines while conducting this research project, and all participants provided informed consent before their involvement. I also declare that I have not plagiarized any content or data during the research process and have taken all necessary measures to ensure that this work is original and follows ethical standards.

I acknowledge and understand that any violation of these ethical guidelines could result in severe consequences, including academic penalties, legal action, and loss of professional reputation.

Dr Alexey Aparin (Anil Sharma)

Joint Institute for Nuclear Research,
Dubna, Russia

Acknowledgements

In completing this project report there is support, guidance and enhancement of many people without those it is not possible to prepare this report. I would like to express my sincere gratitude and appreciation to the following people and organizations who have contributed to the success of my research project titled:

- First and foremost, I would like to thank my project supervisor **Dr Alexey Aparin** for providing guidance and support throughout the entire project. Their insights, feedback, and expertise have been invaluable, and I am grateful for their mentorship.
- I would like to acknowledge the participants of this project who generously gave their time and effort to provide data and insights. Their contributions were essential to the success of this project, and I am indebted to them for their cooperation.
- I would also like to express my gratitude to my friends who provided support, feedback, and encouragement throughout the research process. Their insights and ideas helped to shape this project and contributed to its overall success.
- Finally, I would like to acknowledge the oragnizers of the START programme and the JINR to support this project. Their support has been crucial in enabling the research process and ensuring its success.

I acknowledge that without the support of these individuals and organizations, this research project would not have been possible.

Abstract

Analysis of identified particle production can be a useful to measure the bulk properties of the medium produced in heavy ion collisions at high energies. As a part of preparations for the start of the NICA collider with the MPD experiment designed for the studies of hot and dense nuclear matter, we analyze MC model data on identified particle production at a set of different collision energies. So, we present the measurement of bulk properties of the matter produced in Bi+Bi collisions at $\sqrt{s_{NN}} = 9.2\ GeV$ using the identified hadrons $(\pi^{\pm}), K^{\pm}, proton(p)$ from the MPD experiment at the Nuclotron-based Ion Collider fAcility (NICA). We are using the data of Bi+Bi collisions which is generated with the Monte Carlo generator model named Ultrarelativistic Quantum Molecular Dynamics(UrQMD). We analyze this data using the MpdRoot framework.

Results of Reconstructed tracks, Midrapidity(y), transverse momenta(p_T), distributions of the vertex Z, and distribution of the distance of closest approach(DCA) of the tracks are presented. These results constitute the relations of Energy loss(dE/dx) and total momentum(P) curve to identify the particles, also rapidity and transverse momentum(p_T) plot to figure out the cuts for further analysis.

Contents

List of Figures

1 Introduction

In modern physics, a very challenging task is to investigate hot and dense baryonic matter. This investigation can provide us with very useful information about the in-medium properties of hadrons and nuclear matter equation of state and also can give us an idea of the evolution of the early universe and formation of the neutron stars and other astrophysical objects as well. So to carry out this research, a vast research program of basic sciences is going on over the last two decades. The main centers which are equipped with high energy ion accelerators are GSI Helmholtz Centre for Heavy Ion Research(Germany), The Super Proton Synchrotron - CERN(Geneva), BNL-Relativistic High Ion Collider(USA), and JINR - Nuclotron (Russia).

From the recent observations for the creation of a new kind of Quantum Chromodynamic (QCD) matter and the strongly interacting quark-gluon plasma(SQGP), the theoretical comprehension of these data is far from being complete, which gives us the drive for different laboratories to undertake new efforts in the domain of heavy-ion physics. JINR scientific program is dedicated to the study of hot and dense baryonic matter. To achieve this goal, a new JINR accelerated complex- named the Nuclotron-based Ion Collider fAcility (NICA) [1] has been constructed to provide the heavy ions collisions over a wide range of atomic masses. The NICA collider complex is shown below in figure [1].

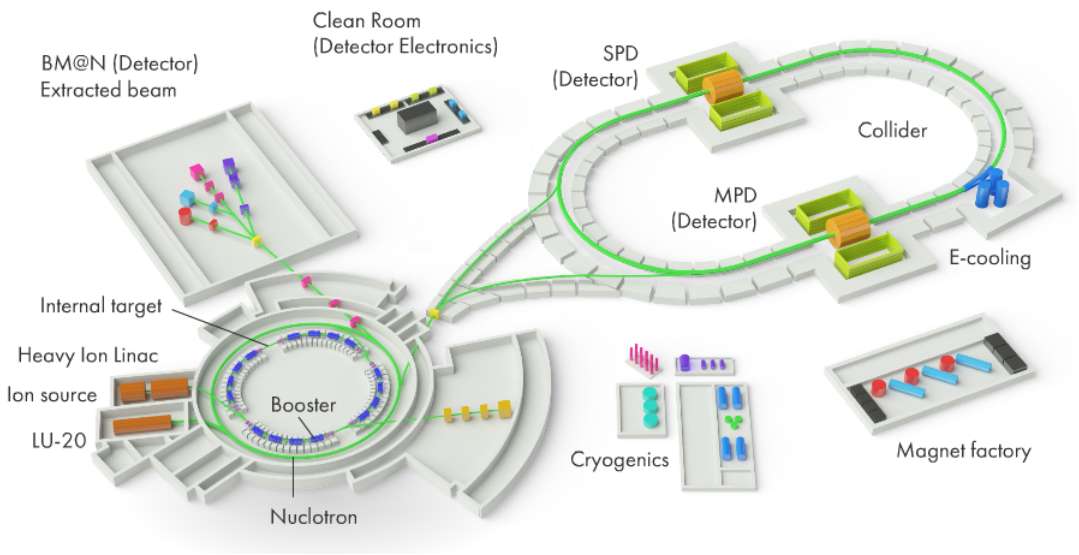

Figure 1: The NICA accelerator complex at JINR.

2 NICA complex and Multi-Purpose detector

This section presents the NICA complex and Multi-Purpose Detector concepts for the international heavy-ion research facility proposed by the JINR to investigate the basic QCD structure of matter [2]. This facility takes into account the broadened scope of the physics of strong interaction and problems related to the fundamental many-body systems and provides particle beams.

2.1 NICA complex

The international mega-science project "NICA complex" is aimed at the study of the properties of nuclear matter in the region of the maximum baryon density. Such type of matter can only exist in the early stages of the evolution of our universe and in the interiors of neutron stars. From the past research done by many scientists about lattice QCD calculations, we can predict both the deconfinement phase transition and chiral symmetry restoration to happen at high energy densities and there is strong experimental evidence that the deconfined phase of nuclear matter or QGP can be created in ultra high energy nuclear collisions [3].

Also, the Experimental data on hadron production properties at SPS(Cern) suggest that this transition occurs within the NICA energy range. In addition, this range is sufficiently large to encompass both, collisions in which the plasma phase is well developed and collisions in which the matter remains purely hadronic throughout. After all of this, the phase diagram of strongly interacting matter contains a critical point and its experimental identification forms a focal point for this research field. Check below the QCD phase diagram in Figure [2].

There are some physics tasks of the NICA heavy-ion program to be studied for different ions by scanning in energy range from 3 to 11 Gev;

- Event-by-event fluctuation in hadron productions (multiplicity, transverse momentum(p_T) etc.
- Femtoscopic correlation.
- Measurements of different flow harmonics for various hadrons.
- Multi-strange hyperon production (including hypernuclei): yield and spectra (the probes of nuclear media phases).
- Photon and electron probes.
- Charge asymmetry.

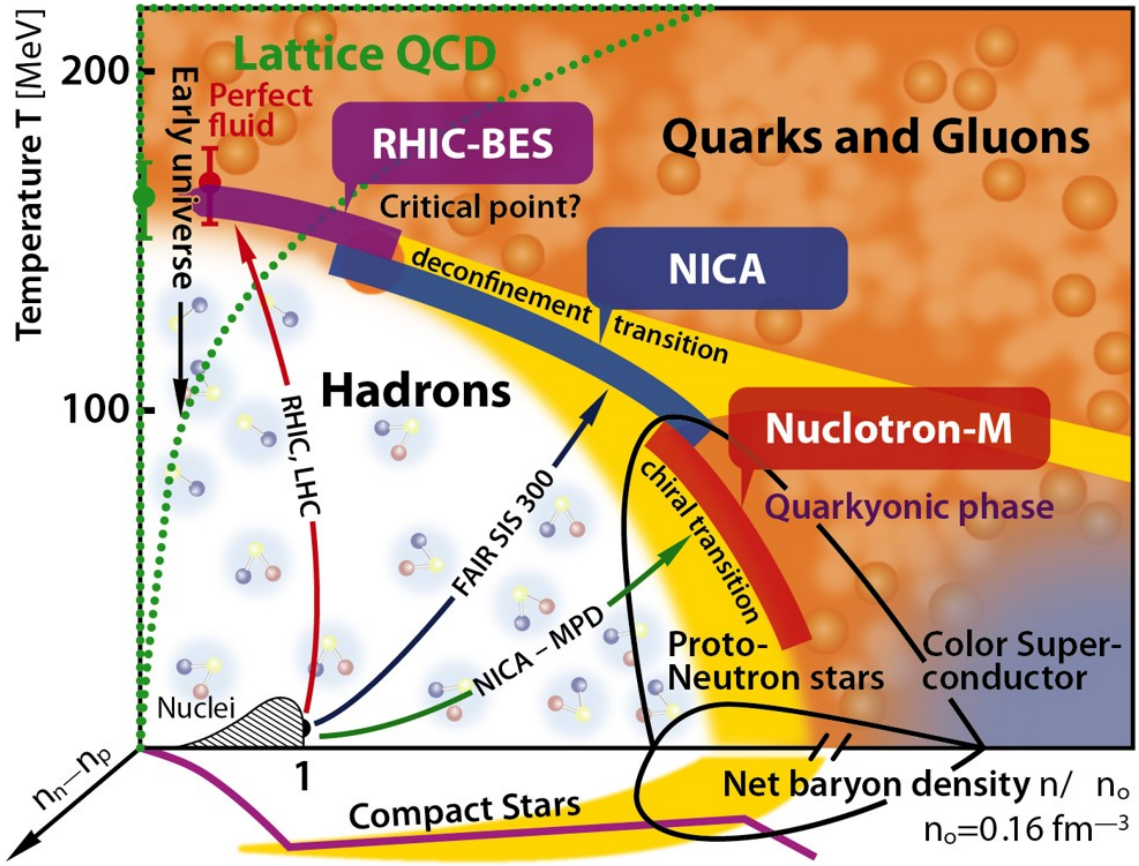

Figure 2: QCD Phase diagram with chemical potential(μ_B) on the horizontal axis and Temperature(T in MeV) on the vertical axis. It shows the regions, where various experiment facilities are working at the present time.

The study of strange particles [4] is of interest because we know from the theoretical predictions that the strangeness enhancement in heavy-ion-induced interactions might be a key to the deconfinement phase transitions. Moreover, nuclear objects with strangeness- hypernuclei can be formed inside the fireball, and since the energy range of the NICA covers the region of the maximal baryon density the production rates of nuclear clusters with strangeness are predicted to be enhanced considerably.

Thus, the outcome of the NICA program, in particular, new experimental data on (anti)hyperon and hypernuclei production which will be taken with the MPD detector will provide valuable insight into the reaction dynamics and properties of the QCD matter [5].

2.2 Multi-Purpose Detector

The main physics experiment at the NICA complex is the Multi-Purpose Detector(MPD) [6] which is operating at the collider. This experimental program includes simultaneous measurements of observables that are presumably sensitive to high nuclear density effects and phase transitions. The software framework for the MPD experiment is MpdRoot, which is based on FairRoot and provides a powerful tool for detector performance studies, development of algorithms for reconstruction, and physics analysis of the experimental data.

For this, We use an extended set of event generators for heavy ion collisions like Ultrarelativistic Quantum Molecular Dynamics (UrQMD), Quark Gluon String Model (QGSM, LAQGSM) etc. The MPD apparatus is shown schematically in Figure [3].

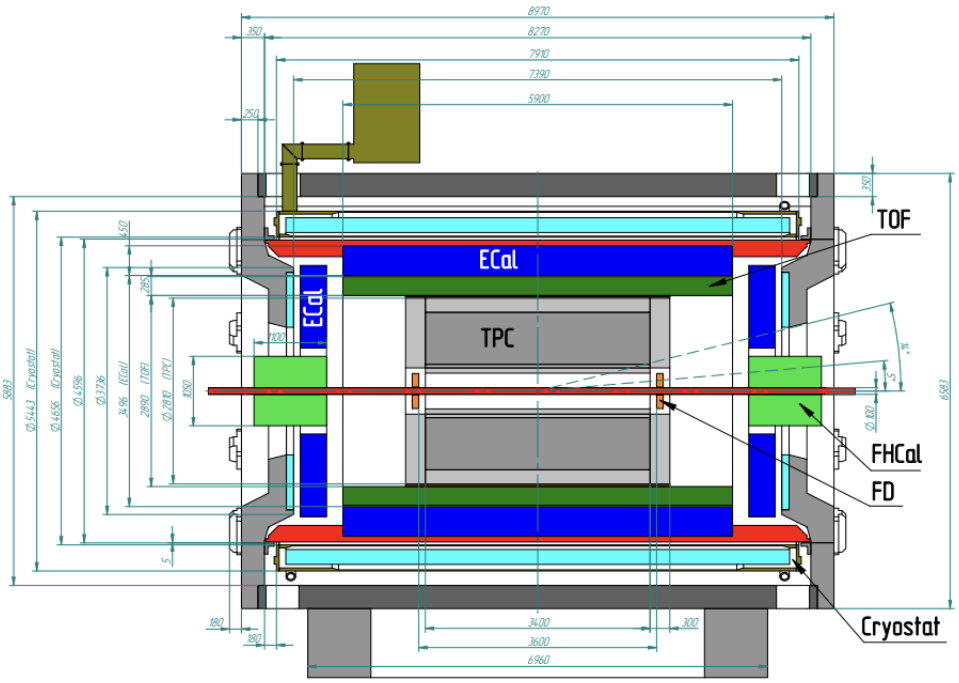

Figure 3: The overall schematic diagram of the multipurpose detector, cross-section by the vertical plane.

The MPD detector has been designed as a 4π spectrometer capable of detecting hadrons, electrons, and photons in heavy-ion collisions at high luminosity. To reach this goal, the detector will comprise a precise 3D tracking system and a high-performance particle identification (PID) system based on time of flight(TOF) measurement and calorimetry. The basic design parameters have been determined taking into account the physics measurements to be performed and several technical constraints guided by a trade-off of efficient

tracking and PID against a reasonable material budget.

In the MPD experiment, the beamline is surrounded by the large gaseous Time Projection Chamber (TPC) which is enclosed by the Time-of-Flight (TOF) barrel. The Electromagnetic Calorimeter (ECal) is placed between the TOF and the MPD magnet. It will be used for the detection of electromagnetic showers and will play the main role in photon and electron measurements. The Fast Forward Detector (FFD) is located in the forward direction within the TPC barrel. It plays the role of a wake-up trigger. The Forward Hadronic Calorimeter (FHCal) is located near the Magnet endcaps. It determines the collision centrality and the orientation of the reaction plane for collective flow studies. The silicon-based Inner Tracker System (ITS) will be installed close to the interaction point in the second stage of the MPD construction. It will greatly enhance tracking and secondary vertex reconstruction capabilities. The miniBeBe detector is placed between the beam pipe and the TPC, close to the beam, and designed to aid in triggering and start time determination for the TOF. The MPD Cosmic Ray Detector (MCORD), installed on the outside of the MPD Magnet Yoke, will measure muons from the cosmic showers.

We are expecting that the MPD will produce event-by-event information on charged particle tracks coming from the primary interaction vertices, together with identification of those particles, and information on the collision centrality. The MPD identification power obtained for charged hadrons with combined mass-squared (m^2) from TOF and energy loss per distance (dE/dx) from TPC [6].

3 Project goals

The project comes under the preparations for the NICA MPD experiment and has the main goal of using MPD software, simulation, and Monte Carlo data to recreate experimental conditions for the Bi+Bi collisions of the MPD experiment at $\sqrt{s_{NN}} = 9.2$ GeV. We are going to obtain the results on transverse momentum(p_T) spectra, position of the event vertex, track selection for TPC, the distance of closest approach (DCA) between each track and the event vertex and then the cuts using the rapidity and total momentum analysis. We also learn the different techniques for particle identification from the energy loss and mass distribution.

4 Data Analysis for Experiment

For the analysis, we are using the simulated data in this project work which was obtained by the Monte Carlo method using the generators UrQMD [7] and undergo the entire chain of reconstruction on the condition of real Bi+Bi collisions of the MPD experiment with the center-of-mass energy of $\sqrt{s_{NN}} = 9.2GeV$. As a software environment, the MPDROOT framework was used. We have a total of 250 original DSTfiles with a total of 124580 Events.

4.1 Event Selection

The criteria for minimum bias-triggered event selection begin with the identification of a primary vertex that is the common point of origin of tracks in an event which is measured by the TPC. In order to reject the background events, which involve interactions with the beam pipe of radius 6 cm, the event vertex radius is required to be within 4 cm of the center of the MPD detector. The ring of a black dense area of data points in figure [4] corresponds to collisions between the beam nuclei and the beam pipe. This type of background is more significant and useful in low-energy data.

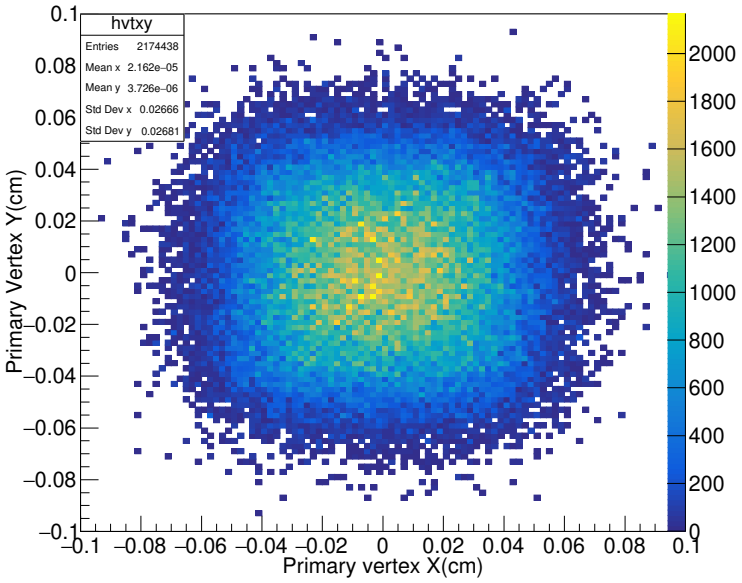

Figure 4: The event vertex x and y of the reconstructed event in Bi+Bi collisions at $\sqrt{s_{NN}} = 9.2GeV$.

The distributions of the primary vertex position along the longitudinal (beam) direction (V_z) are shown in figure [5] for 9.2 GeV Bi+Bi collisions. The

wide z-vertex distribution at lower energies is due to the fact that the beams are more difficult to focus on. Only those events which have a V_z within 50 cm were selected for the analysis. These values are chosen to achieve uniform detector performance and sufficient statistical significance of the measured observable.

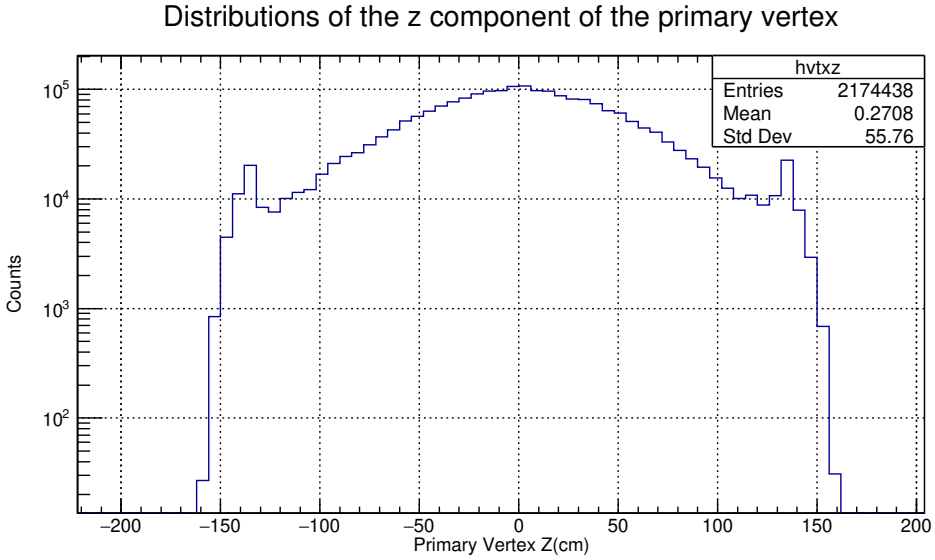

Figure 5: The distributions of the z component of the primary vertex in Bi+Bi collisions at $\sqrt{s_{NN}} = 9.2GeV$.

4.2 Centrality Selection

Centralities in Bi+Bi collisions at $\sqrt{s_{NN}} = 9.2GeV$ is defined by using the number of primary charged-particle tracks reconstructed in the TPC. This is generally called the reference multiplicity as well. The centrality classes are obtained as fractions of the reference multiplicity distribution. The events are divided into the following centrality classes: 0-5%, 5-10%, 10-20%, 20-30%, 30-40%, 40-50%, 50-60%, 60-70%, and 70-80%, in figure [6].

4.3 Track Selection

Track selection criteria are necessary for analysis. The tracks that extrapolate to TOF active cells have already been selected for the number of hits criteria [8]. In figure [7], we can see that tracks must have at least 10 points used in track fitting out of the maximum of 53 hits possible in the TPC. To prevent multiple counting of split tracks, at least 19% of the total possible fit points are required.

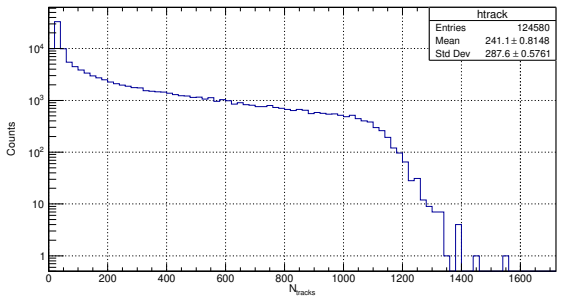

Figure 6: The distributions of the tracks in Bi+Bi collisions at $\sqrt{s_{NN}} = 9.2GeV$.

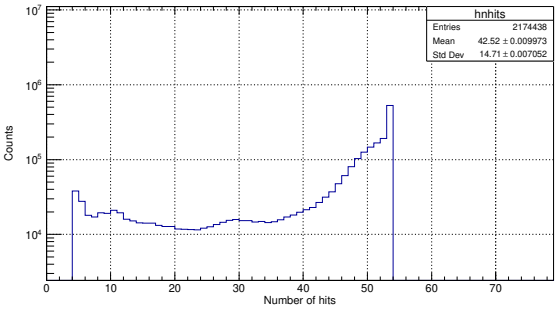

Figure 7: Plot of the Number of hits which is showing the minimum(10) and maximum(53) number of hits for Bi+Bi collisions at $\sqrt{s_{NN}} = 9.2GeV$.

In order to suppress the admixture of tracks from secondary vertices, a requirement of less than 3 cm is placed on the distance of the closest approach (DCA) between each track and the event vertex. We can clearly see this in our DCA plot, in figure [8].

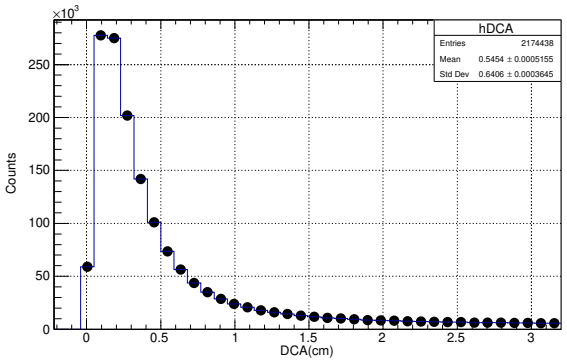

Figure 8: The distributions of the DCA in Bi+Bi collisions at $\sqrt{s_{NN}} = 9.2GeV$.

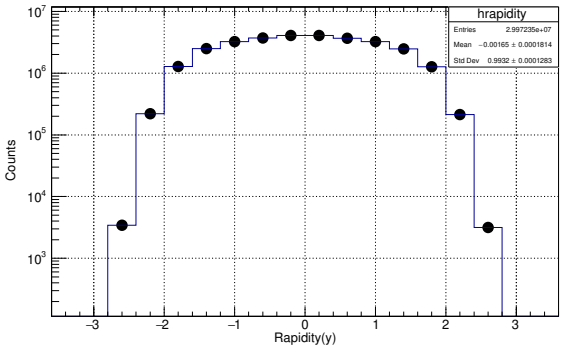

Figure 9: Plot of the rapidity in Bi+Bi collisions at $\sqrt{s_{NN}} = 9.2GeV$.

Now let's discuss Rapidity [9]: Pseudorapidity is a useful quantity because it is related to the rapidity of a particle, which is a quantity that is invariant under Lorentz transformations in the longitudinal direction. Rapidity is defined as:

$$y = \frac{1}{2} log\left[\frac{P_{tot} + p_z}{P_{tot} - p_z}\right] \tag{4.3.1}$$

where P_{tot} is the total momentum of the particle and p_z is its momentum along the beam axis. As we know already Pseudorapidity describes the distributions of particles, which we can see in figure [9]. So we need to select a constant region to study and for analysis. That's why, we are doing the cuts for

rapidity in the $|y| < 0.1$ region. And we will be going to keep the same track cuts for all energies.

4.4 Particle Identification

4.4.1 Energy loss distribution technique

Particle identification is accomplished in the TPC by measuring the energy loss (dE/dx). Figure [10] shows the energy loss dE/dx of measured charged particles plotted as a function of rigidity which is the fraction of momentum and charge of the particles. It can be seen that the TPC can identify pions ($\pi^{\pm}$), kaons ($K^{\pm}$), and protons (p) antiprotons ($\bar{p}$) at low momentum as illustrated by the color bands, fig. [11], [12], and [13]. We also use time of flight information to identify particles with higher momentum. The TOF particle identification for this analysis used above $p_T = 0.4GeV/c$.

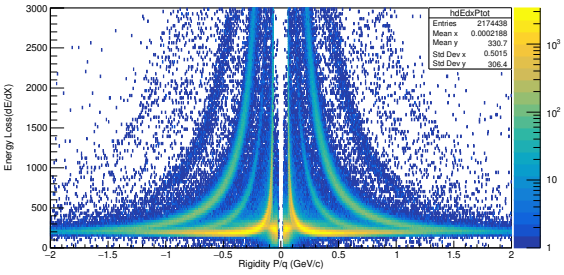

Figure 10: The dE/dx of charged tracks with the rigidity(P/q) for Bi+Bi collisions at $\sqrt{s_{NN}} = 9.2GeV$ at rapidity $|y| < 0.1$ for all the particles.

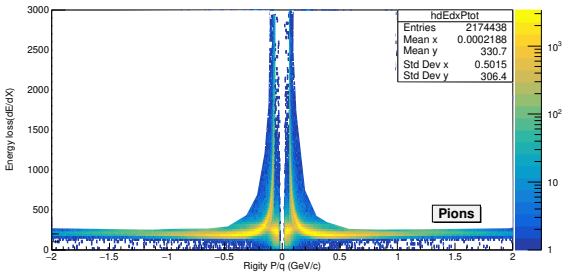

Figure 11: The dE/dx of charged tracks with the rigidity(P/q) for Bi+Bi collisions at $\sqrt{s_{NN}} = 9.2GeV$ at rapidity $|y| < 0.1$ only for pions.

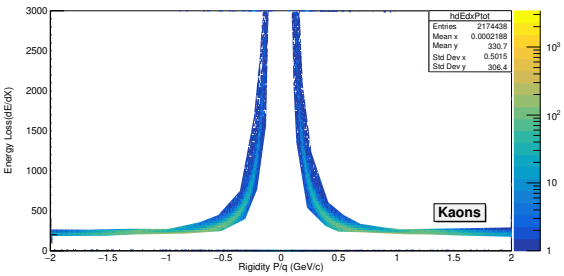

Figure 12: The dE/dx of charged tracks with the rigidity(P/q) for Bi+Bi collisions at $\sqrt{s_{NN}} = 9.2GeV$ at rapidity $|y| < 0.1$ only for kaons.

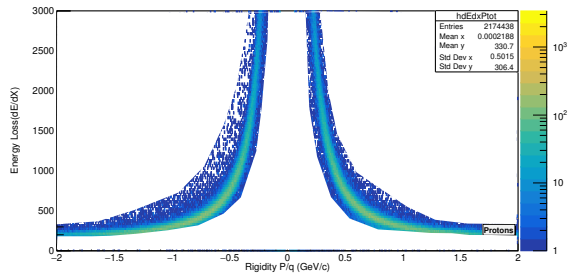

Figure 13: The dE/dx of charged tracks with the rigidity(P/q) for Bi+Bi collisions at $\sqrt{s_{NN}} = 9.2GeV$ at rapidity $|y| < 0.1$ only for protons.

So now to get the information for the interacting particles, we will take slices of the x-axis or the momentum axis for different ranges. As you can

see, fig.[14], that the peaks for all three particles(pions, kaons, protons) are distinguishable or well separated and easy to analyze for low momentum $p_T = 0.30 - 0.34 GeV/c$. But as we go for higher and higher momentum all three peaks, which correspond to all different particles, are getting overlapped into one so at higher momentum, it's difficult to distinguish the particles, fig. [15], [16], [17], [18], and [19]. See the table [1], for interacting particles for all the different ranges of momentum.

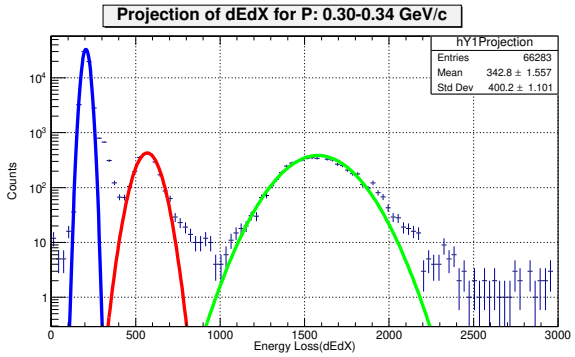

Figure 14: The slice of energy loss(dE/dx) in the momentum range 0.30-0.34 GeV/c for pions(blue line), kaons(red line), and protons(green line).

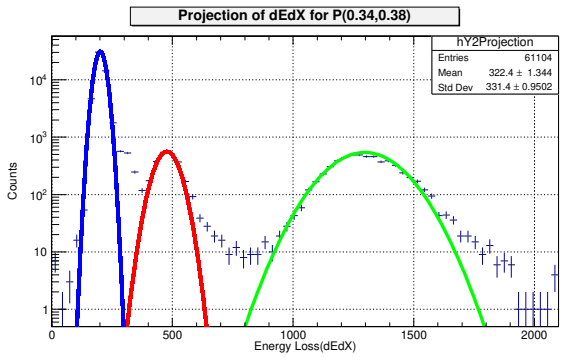

Figure 15: The slice of energy loss(dE/dx) in the momentum range 0.34-0.38 GeV/c.

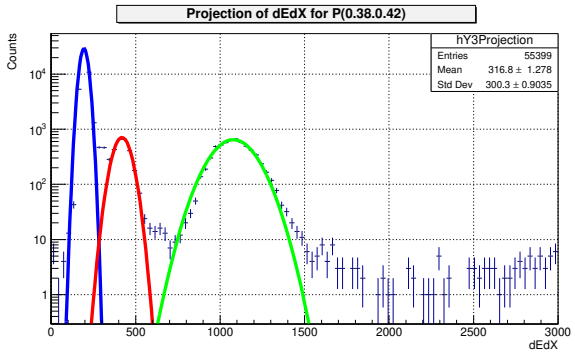

Figure 16: The slice of energy loss(dE/dx) in the momentum range 0.38-0.42 GeV/c.

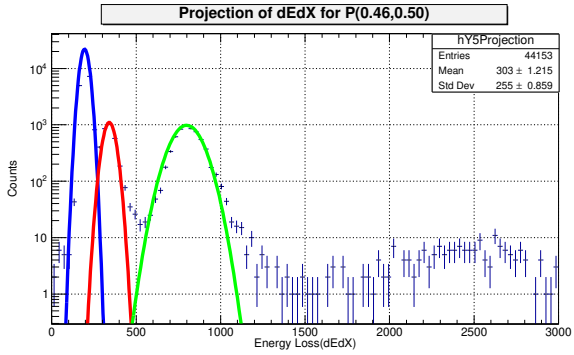

Figure 17: The slice of energy loss(dE/dx) in the momentum range 0.46-0.50 GeV/c.

Figure [20] shows the inverse of particle velocity in the unit of the speed of light $1/\beta$ as a function of rigidity. The expectation values for pions, kaons, and protons are shown as the curves. As we can see in this figure, there is a band representing $1/\beta < 1$ or $1/\beta > 1$ at low momentum. This nonphysical band is occurring here because of the charged hadron and a photon-converted electron hitting in the same TOF cluster.

This conversion may happen in the TPC outer field cage or box. Due to high

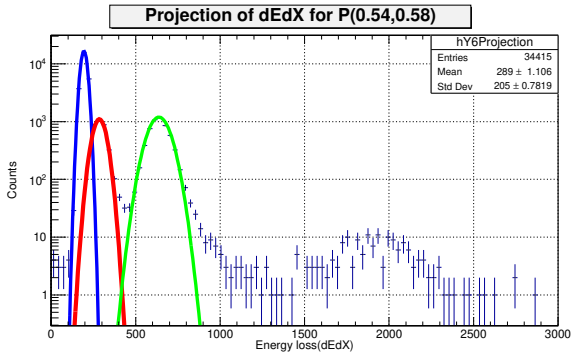

Figure 18: The slice of energy loss(dE/dx) in the momentum range 0.54-0.58 GeV/c.

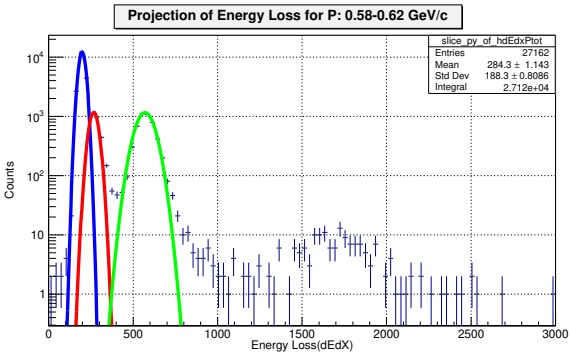

Figure 19: The slice of energy loss(dE/dx) in the momentum range 0.58-0.62 GeV/c.

	Number of Particles		
Momentum range in GeV/c	Pions	Kaons	Protons
0.30-0.34	1658808	65450	168463
0.34-0.38	1622853	74179	179880
0.38-0.42	1584232	81875	185195
0.46-0.50	1296064	87839	197131
0.54-0.58	753475	99919	178714
0.58-0.62	585926	75934	151818

Table 1: Total number of particle interacting in the collisions for different momentum ranges.

occupancy, these TOF hits are accidentally matched to hadrons tracks in the TPC and resulting in the wrong time of flight. They have a negligible effect on charged hadron yields.

4.4.2 Mass^2 distribution technique

The raw yields from the TOF are obtained by using the variable mass square(m^2), which is given by:

$$m^2 = p^2\left(\frac{c^2T^2}{L^2} - 1\right)$$

where p, T, L, and c are the momentum, time of travel by the particle, path length, and speed of light, respectively. In figure [21], we can see the m^2 distribution and momentum plot, where we can identify the particles as well. There is pions ($\pi^{\pm}$) for lower mass region($0.0-0.1 GeV/c^2$), kaons ($K^{\pm}$) for mass region($0.2-0.3 GeV/c^2$), and protons (p) antiprotons ($\bar{p}$) for mass region($0.7-1.0 GeV/c^2$), fig. [22], [23], and [24].

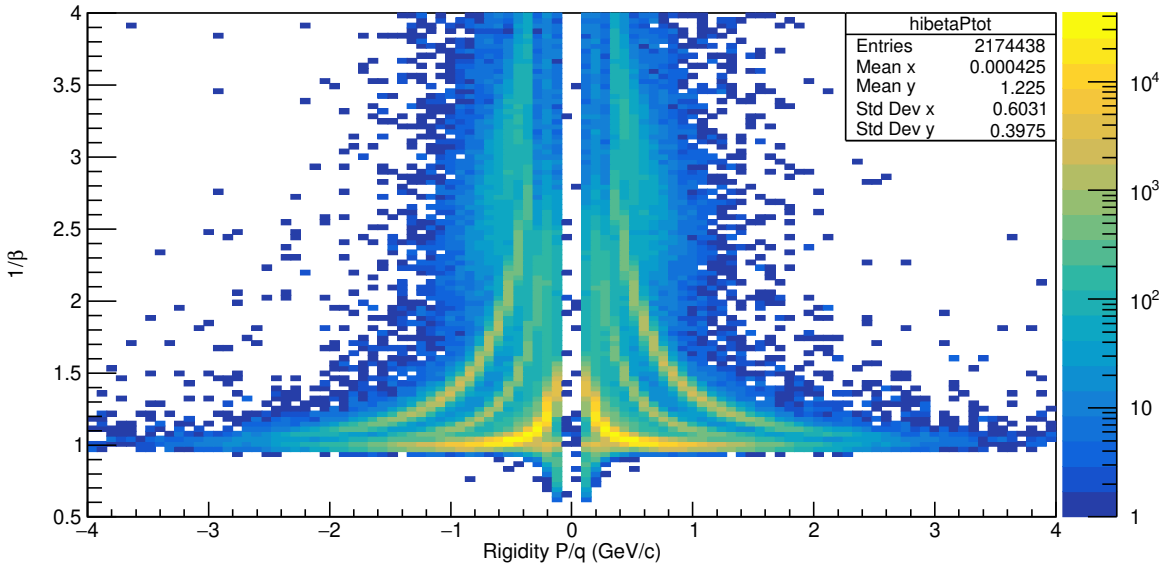

Figure 20: The plot of $1/\beta$ with the rigidity(P/q) for Bi+Bi collisions at $\sqrt{s_{NN}} = 9.2GeV$ at rapidity $|y| < 0.1$ for all the particles.

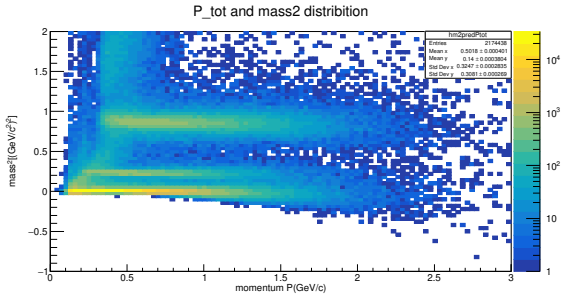

Figure 21: The plot of m^2 with the momentum for Bi+Bi collisions at $\sqrt{s_{NN}} = 9.2GeV$ at rapidity $|y| < 0.1$ for all the particles.

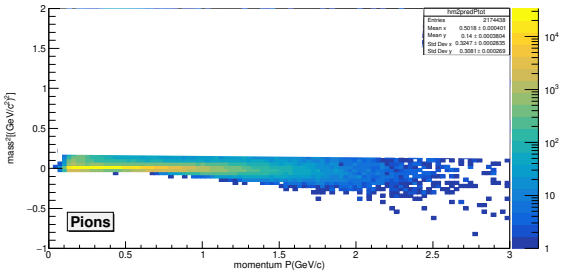

Figure 22: The plot of m^2 with the momentum for Bi+Bi collisions at $\sqrt{s_{NN}} = 9.2GeV$ at rapidity $|y| < 0.1$ only for pions.

So now to get the information for the interacting particles, we will take slices of the x-axis or the momentum axis for different ranges for mass square distributions. As you can see, fig.[25], the peaks for all three particles(pions, kaons, protons) are distinguishable or well separated and easy to analyze for low momentum $p_T : 0.7 - 0.8\ GeV/c$. But as we go for higher and higher momentum all three peaks, which correspond to all different particles, are getting merged into one so at higher momentum.

The m^2 distributions are obtained for rapidity $|y| < 0.1$ for all the particles in different p_T ranges as shown in the fig. [26], [27], and [28].

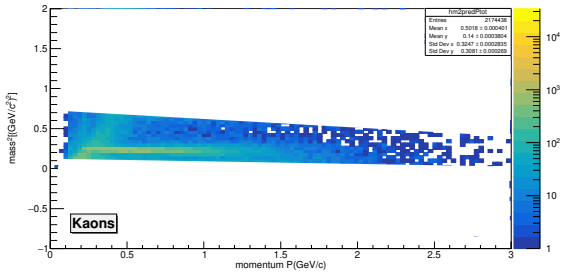

Figure 23: The plot of m^2 with the momentum for Bi+Bi collisions at $\sqrt{s_{NN}} = 9.2GeV$ at rapidity $|y| < 0.1$ only for kaons.

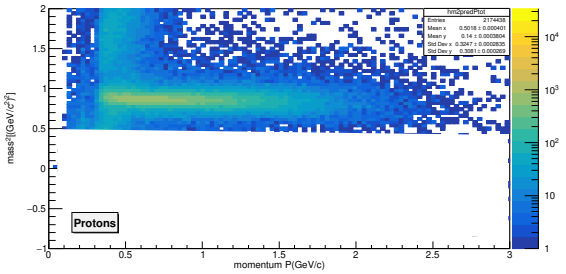

Figure 24: The plot of m^2 with the momentum for Bi+Bi collisions at $\sqrt{s_{NN}} = 9.2GeV$ at rapidity $|y| < 0.1$ only for protons.

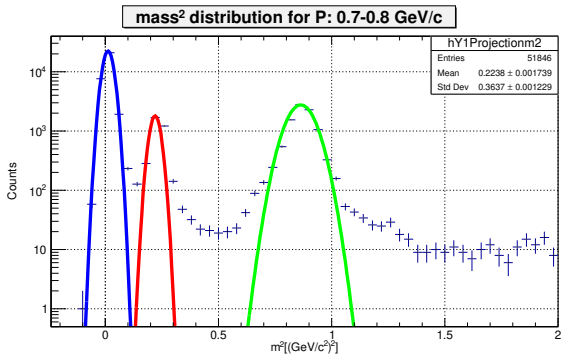

Figure 25: The slice of m^2 in the momentum range 0.7-0.8 GeV/c for pions(blue line), kaons(red line), and protons(green line).

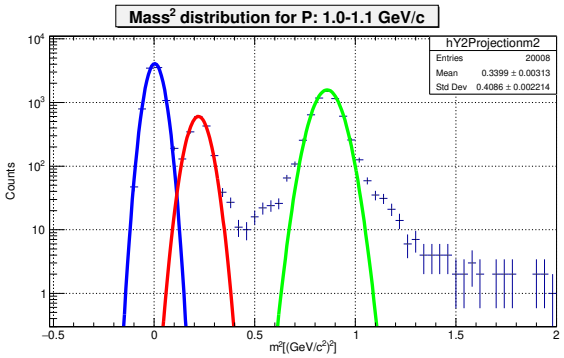

Figure 26: The slice of m^2 in the momentum range 1.0-1.1 GeV/c.

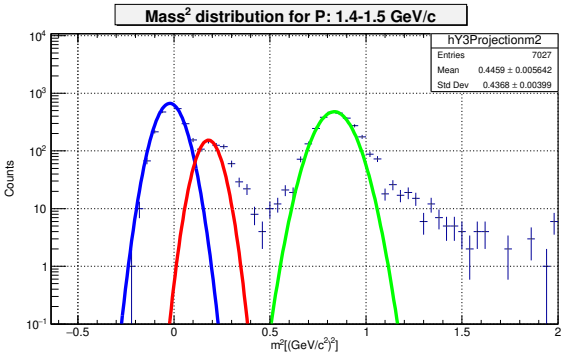

Figure 27: The slice of m^2 in the momentum range 1.4-1.5 GeV/c.

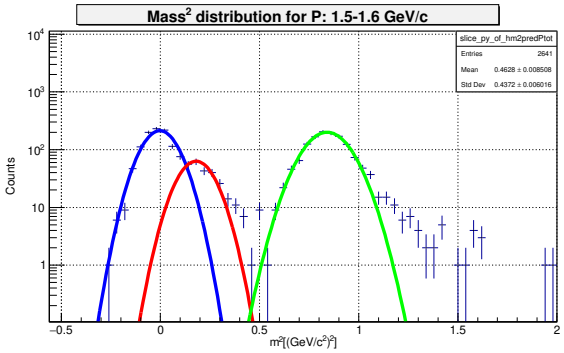

Figure 28: The slice of m^2 in the momentum range 1.5-1.6 GeV/c.

4.5 TPC Acceptance

Finally, for TPC acceptance, the selection criteria and needed cuts for all energies are:

- Number of hits/points, $N_{hits} > 25$,
- Only charged particles taken in account,
- Rapidity, $|y| < 0.1$,
- Primary vertex Z < 50 cm,
- Distance of closest approach(DCA) < 3 cm,
- Bi+Bi collisions for the center of mass energy $\sqrt{s_{NN}} = 9.2GeV$ using the generator UrQMD.

5 Discussion and Future scope of work

In this project, Monte Carlo data of Bi+Bi heavy ion collisions in the center-of-mass energy range is analyzed $\sqrt{s_{NN}} = 9.2GeV$. Also, several other studies have been performed to improve the quality of particle identification using energy loss and mass square distribution and made some cuts for better results or analysis like DCA cuts, rapidity cuts, the minimum number of hits, etc. From these cuts and analysis, we got the spectra for transverse momenta (p_T), in Figure [29] (without cuts), [30] (with cuts). For further analysis, it is necessary to analyze more statistical data using different Monte Carlo models for different values of the collision energy of the center of mass etc.

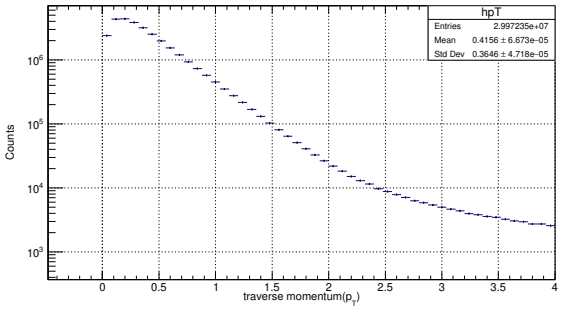

Figure 29: Plot of transverse momentum(p_T) spectra for Bi+Bi collisions at $\sqrt{s_{NN}} = 9.2GeV$.

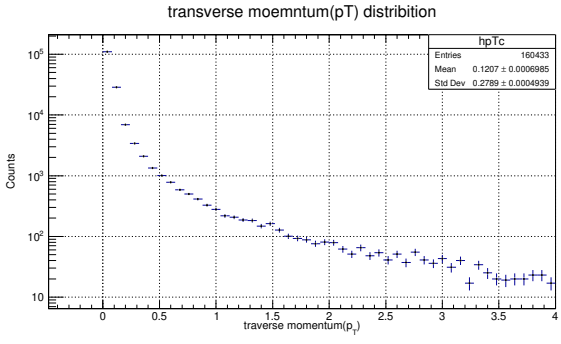

Figure 30: Plot of transverse momentum(p_T) spectra for Bi+Bi collisions at $\sqrt{s_{NN}} = 9.2GeV$ with cuts at $|y| < 0.1$.

For future scope, we are aiming to contribute to the studies of bulk properties of this system for an incoming run of the MPD/NICA experiment. For preliminary results of the first runs on the NICA complex with Bi+Bi heavy ion collisions at low energies, previously done studies of first physics are necessary. This work can lead us to the chemical and kinetic freeze-out dynamics at these energies. That's why, I am looking forward to visiting the JINR facility for further work. There, we can also work on centrality dependence for particle production, particle yields, particle ratio, the energy dependence of particle production, and freeze-out parameters. In the end, we can find out the relation of temperature(T) and chemical potential(μ_B) for the phase diagram to search for the QCD critical point.

References

[1] Website for nica complex facility, https://nica.jinr.ru/.

[2] I. Arsene and I.G. Bearden et. al. Quarkgluon plasma and color glass condensate at rhic, the perspective from the brahms experiment. *Nuclear Physics A*, 757(1):1–27, 2005. First Three Years of Operation of RHIC.

[3] M. S. Abdallah et al. Pion, kaon, and (anti)proton production in U+U collisions at $\sqrt{s_{NN}}$=193 GeV measured with the STAR detector. *Phys. Rev. C*, 107(2):024901, 2023.

[4] J. Adam and et. al. Adamczyk. Strange hadron production in Au + Au collisions at $\sqrt{s_{NN}} = 7.7$, 11.5, 19.6, 27, and 39 gev. *Phys. Rev. C*, 102:034909, Sep 2020.

[5] L. Adamczyk and et. al. Adkins. Bulk properties of the medium produced in relativistic heavy-ion collisions from the beam energy scan program. *Phys. Rev. C*, 96:044904, Oct 2017.

[6] V. Abgaryan and Acevedo Kado et. al. Status and initial physics performance studies of the mpd experiment at nica. *The European Physical Journal A*, 58(7), July 2022.

[7] Urqmd official website, https://urqmd.org/.

[8] R. Debbe. Time of flight track matching efficiency in star experiment, https://drupal.star.bnl.gov/STAR/files/userfiles/2729/file/TOFmatchingNote.pdf.

[9] Dr.ssa Barbara Guerzoni. Identified primary hadron spectra with the tof detector of the alice experiment at lhc, https://cds.cern.ch/record/1495621/files/tesiGuerzoniDottorato.pdf.